Nuclear Metabolism of Ribosomal RNA in Growing, Methionine-Limited, and Ethionine-Treated HeLa Cells†

Stanley F. Wolf and David Schlessinger*

ABSTRACT: As the first step to provide a quantitative method for determining the points of regulation of net ribosomal RNA synthesis in mammalian cells, the approach to steady-state labeling of individual pre-rRNA and rRNA species with [^{3}H]methylmethionine was determined in logarithmically growing HeLa cells. Data from polyacrylamide gel profiles were analyzed on an IBM 360 computer with a simulation, analysis, and modeling program (SAAM 23). In HeLa cells doubling every 25 to 28 h, 1.4% of a total of about 8×10^6 rRNA sequences was in the form of pre-rRNA; the half-lives for processing of 45S, 32S, and 20S pre-rRNA were 10, 25, and 2 min, respectively. The kinetics predicted steady-state levels of ribosomes, and ratios of 45S/32S pre-rRNA, that were directly verified, as was the prediction of a fraction of 45S pre-rRNA that was relatively slowly methylated. A comparison of the results from experiments with spinner and plate cultures indicated no difference in processing pathways or processing rates between the two. Every methyl group incorporated into 45S pre-rRNA in the growing cells could be accounted for and later appeared in mature rRNA; i.e., there was little or no nuclear degradation of 18S or 28S sequences in pre-rRNA ("wastage"). In contrast, in cells treated with ethionine, little mature 28S or 18S rRNA accumulated, although the peak of 45S rRNA was nearly normal, and substantial amounts of 32S also appeared. Thus, as was also suggested by kinetic analysis, methylation is apparently not essential for correct initial cleavages of 45S pre-rRNA, but is required for the later steps in rRNA processing.

Regulation of cellular ribosome content may be exercised at several levels between the synthesis of the initial 45S pre-rRNA[1] transcript and the accumulation of completed 60S and 40S subunits in the cytoplasm. During its maturation, approximately 50% of the primary pre-rRNA transcript of HeLa cells is cleaved or trimmed away (see Maden, 1971, for a review). In some cases, it has been suggested that even entire pre-rRNA transcripts may be degraded or "wasted" before the rRNA has the opportunity to function in the cytoplasm (Cooper, 1973; Cooper and Gibson, 1971). However, estimates of the rates of processing of the ribosomal precursors and of any wastage in the nucleus have remained qualitative (Soeiro et al., 1968; Abelson et al., 1974).

To establish a method for determining the rates of formation and amounts of each of the nuclear pre-rRNA and cytoplasmic rRNA species, and hence to look at the possible control points in ribosome synthesis, we have refined the approach to steady-state labeling analysis using methylmethionine as a precursor of RNA methyl groups and a simulation, analysis, and modeling program (SAAM 23). We have thereby been able to maintain the cultures in a nearly normal physiological state during the course of a typical experiment while avoiding many of the experimental problems of pulse labeling and pulse chase experiments with labeled nucleosides.

Experiments with suspension and plate cultures of HeLa cells demonstrated the utility of the method. Negligible wastage of newly formed nuclear pre-rRNA was found in logarithmically growing cultures. In addition, the analysis detected the existence of a significant fraction of undermethylated 45S pre-rRNA even in cells growing in substantial levels of methionine. To investigate further the relation between methylation and rRNA processing, cells were studied in the presence of ethionine. The analogue blocks RNA methylation, but does not significantly inhibit rates of protein synthesis. Consistent with the kinetic results, cells labeled in the presence of ethionine accumulated 45S and 32S RNA species at nearly normal rates, but failed to produce 28S or 18S rRNA.

Experimental Procedure

Cell Culture and Collection. HeLa S3 cells were maintained (1) in spinner culture in log phase growth at 37 °C in Joklik MEM (Gibco) supplemented with 5% horse serum (Kansas City Biologicals) at a concentration between 2×10^5 and 4×10^5 cells/mL; or (2) grown in T flasks in MEMα supplemented with 10% fetal calf serum (Kansas City Biologicals), splitting the cultures approximately every third day.

In preparation for a labeling experiment, cells grown in spinner culture were centrifuged for 10 min at 2000g and resuspended directly at 10^6 cells/mL in prewarmed Joklik MEM lacking methionine, and fortified with 5% dialyzed horse serum (Gibco).

Cells grown in T flasks were scraped off the substrate with a rubber policeman and plated on 60-mm Petri dishes at approximately 7.5×10^5 cells/plate in MEMα supplemented with 10% dialyzed fetal calf serum (Gibco). On the morning of an experiment (approximately 48 h after plating), cells on Petri dishes were transferred to a closed hood maintained at 37 °C, 5% CO_2, and 80% relative humidity. The medium was aspirated off; the cell monolayer was washed with 3 mL of prewarmed MEMα supplemented with 10% dialyzed fetal calf serum which had been adjusted to the desired methionine concentration and equilibrated with 5% CO_2; 3 mL more of the same medium was added.

† From the Department of Microbiology and Immunology, Division of Biology and Biomedical Sciences, Washington University School of Medicine, St. Louis, Missouri 63110. *Received November 23, 1976.* This research was supported by National Institutes of Health Grant GM 21357. Access to the IBM 360 and SAAM 23 program was through the Washington University Biomedical Computer Lab and supported by the National Institutes of Health Grant RR 05389.

[1] Abbreviations used: pre-rRNA, ribosomal precursor RNA; EDTA, (ethylenedinitrilo)tetraacetic acid; Trizma base or Tris, 2-amino-2-hydroxymethyl-1,3-propanediol; PCA, perchloric acid; MEM, minimum essential medium.

To inhibit incorporation of methyl label by de novo synthesis of bases, all washing, preincubation, and labeling media contained sodium formate at a final concentration of 0.02 M, adenosine, at 2×10^{-5} M, and guanosine, at 2×10^{-5} M (Maden et al., 1972).

Labeling. Except where noted otherwise, all labeled nucleotides and amino acids were from New England Nuclear Corp.

(1) Spinner Cultures. A stoppered flask containing the resuspended cells equilibrated at pH 7.2 with 5% CO_2–95% air was placed in a shaking water bath maintained at 37 °C for 20 to 30 min before labeling. Label and growth inhibitors were then added as described in the figure legends. Samples were collected by pipetting portions of the culture into tubes containing an equal volume of crushed frozen solution A (0.27 M NaCl–0.005 M KCl–0.016 M Na_2HPO_4–0.002 M KH_2PO_4, pH 7.4) and sufficient 1 M $CaCl_2$ to yield a final concentration of 2 mM Ca^{2+}. The cells were centrifuged, resuspended in ice-cold solution A, and centrifuged again. The cell pellet was then suspended in 4 mL of ice-cold distilled water per 10^7 cells and ⅕ volume of 5× extraction buffer (0.5 M Trizma base–0.05 M EDTA–2.5% sodium dodecyl sulfate; adjusted with acetic acid to pH 5.4) was added. The cells were vortexed quickly, and an equal volume of phenol saturated with extraction buffer lacking sodium dodecyl sulfate was added. In each experiment, the lysed cells were stored at 0 °C until all the samples had been collected.

(2) Monolayer Cultures. The washed cells were allowed to preincubate in the fresh low methionine medium for 1 to 2 h. To start the labeling, the preincubation medium was aspirated off and 1.5 mL of the same medium containing [^{3}H]methylmethionine was added as described in the figure legends. Samples were collected by aspirating off the labeling medium and placing the Petri dish on ice. The monolayer was then rinsed with 3 mL of ice cold solution A containing 2 mM Ca^{2+}. Two milliliters of ice-cold extraction buffer was added and the plates were swirled until the cells had lysed. The lysate was transferred to a centrifuge tube, the plate was washed with 2 mL more of ice-cold extraction buffer, and the lysates were combined and vortexed. An equal volume of phenol prewarmed to 70 °C and saturated with extraction buffer lacking sodium dodecyl sulfate was added and the lysate vortexed again. Samples were stored on ice until all the time points had been taken.

RNA Extraction. The RNA was phenol extracted once at 55 °C by vigorous shaking in a heated water bath for 5 min. The aqueous and phenol phases were separated by centrifugation and the aqueous phase was pipetted into a fresh test tube and stored at 0 °C. The phenol phase and interface were reextracted by vortexing with ½ volume of ice-cold extraction buffer, and this second aqueous phase was combined with the first. The combined aqueous phases were extracted with ½ volume of phenol–chloroform–isoamyl alcohol (1:1:1%). The final aqueous phases were precipitated with 2 to 2.5 volumes of 95% ethanol, containing 0.15 M sodium acetate, and stored overnight at −20 °C. The samples were then resuspended in 1 mL of extraction buffer and phenol extracted as described above, except that all steps were done at 0 °C. (These additional extractions after the first ethanol precipitation were one of the precautions found to be necessary to remove traces of protein and to prevent any aggregation of the RNA, which would then remain at the top of polyacrylamide gels during analytical electrophoresis. Another precaution was the use of 0.5% sodium dodecyl sulfate in the extraction buffer. This concentration was found to be optimal in adequately inhibiting nucleases. Higher levels of detergent led to extraction of much more DNA and to higher, variable levels of aggregation during electrophoresis.) The final aqueous phases were again precipitated with 2 to 2.5 volumes of 95% ethanol containing 0.15 M sodium acetate and stored overnight at −20 °C. On the following day the samples were washed twice with 70% ethanol and resuspended in 0.5 mL of extraction buffer. Two portions from each sample were taken. One was diluted into 0.1 N NaOH and the absorbance at 260 nm measured; the other was counted. The measured absorbance and cpm were used to calculate the specific activity of the RNA in each sample. The samples were again precipitated with 2 to 2.5 volumes of 95% ethanol, containing 0.15 M sodium acetate, and stored overnight at −20 °C.

In preparation for polyacrylamide gel electrophoresis, the samples were resuspended in 50 to 100 μL of 0.01 M sodium acetate–0.001 M EDTA–0.5% sodium dodecyl sulfate in 90% formamide (the use of Tris–acetate buffer at this point caused aggregation of the RNA). A portion of each sample was counted. Bromophenol blue, 0.1%, and marker ^{14}C-labeled *E. coli* ribosomal RNA were then added to the rest. The samples were warmed at 55 °C for 5 min and chilled rapidly to 0 °C, and a measured volume was applied to the polyacrylamide gels.

Polyacrylamide Gel Electrophoresis. The technique used for acrylamide gel electrophoresis was essentially that of Weinberg and Penman (1968), with the following modifications: gels 13.5 cm long were used, containing 2.2% acrylamide, 0.25% diacrylate (v/v), and 10% glycerol. The gels were made the day before use and run at 4 °C at 5 mA/gel constant current for 8 h. The entire length of the gel was submerged in the lower electrolyte tank, and the buffer was stirred during electrophoresis to ensure that the gels remained cool.

After electrophoresis, gels were frozen and sliced into 1.8-mm slices, and the slices were dissolved overnight at 37 °C in capped vials containing 1 mL of 10% protosol (New England Nuclear Corp.) dissolved in toluene scintillator. Four milliliters more of toluene scintillator was then added to each vial and the samples were counted with settings to permit simultaneous determinations of ^{3}H and ^{14}C. The cpm in various RNA species were then summed for each gel and analyzed as outlined in Results.

Modeling, Half-Life, and Pool Size Calculations. A model is submitted to the SAAM 23 program by specifying (1) an initial estimate of the rate constant ($\lambda_{a,b}$) for each pathway from component "b" to component "a" in the model; (2) the initial conditions (e.g., in all models shown, the number of labeled molecules in all RNA pools at zero time was set to zero and the initial number of [^{3}H]methylmethionine molecules was set to a very high value); (3) the data for the experiment; and (4) error estimates for the data. Dependence relations may also be submitted. For example, the rate constant for one pathway can be made dependent on the rate constant for another pathway (e.g., in all the models shown $\lambda_{20,45}$ was set equal to $\lambda_{32,45}$ and in addition, in model C (Table I), $\lambda_{20,M}$ was set equal to $\lambda_{32,M}$). It is also possible to include certain constraints. For example, in model B (Table I) the total number of labeled molecules in pool 45_a and 45_b at time t was constrained to be equal to the number of 45S molecules at that time. When desired, wastage pathways are included by submitting a rate constant for a pathway with no normal product. The program then iteratively adjusts the rate constants until further adjustments decrease the sum of squares of the difference between the calculated and observed values by less than 1%. At that point, the model is assumed to have converged and the

computed data are printed out.

The half-life of a species is determined from the rate constants calculated by the program using:

$$T_{1/2} \text{ of species "x"} = \frac{\ln 2}{\sum_b \lambda_{b,x}}$$

The relative and absolute pool sizes of pre-rRNA and rRNA species were calculated using the rate constants computed by the SAAM 23 program with model A of Table I. The relative pool sizes were calculated by solving the differential equations for the model (see Results) at the steady-state limit. At that time, $dq/dt = 0$ and the equations reduce to a simple algebraic relationship. Computed rate constants can then be used to solve for q_a, q_b . . . etc. The level of 32S pre-rRNA was arbitrarily set equal to 1 and the other pool sizes were calculated relative to the 32S species.

The absolute pool sizes were calculated from the relative pool sizes and an estimate of the specific activity of the [^{3}H]methylmethionine during the labeling.

Determination of the RNA Content Per HeLa Cell. HeLa S3 cells were grown logarithmically as described above. Samples containing cells at a known concentration were collected and macromolecules precipitated at 0 °C by adding perchloric acid (PCA) to a final concentration of 0.2 N. The precipitated material was washed twice by centrifugation in 0.2 N PCA at 0 °C. The final pellet was resuspended in 0.3 N KOH, incubated at 37 °C for 1 h, and acidified to a final concentration of 0.2 N PCA, and the acid-insoluble material was precipitated at 0 °C. The precipitated material was pelleted and washed twice more by centrifugation in 0.2 N PCA, and the three supernatants were combined. The RNA content of the combined supernatants was determined using the orcinol reaction as described by Dische (1953).

Estimation of the Cellular Methionine Pool and Methionine Specific Activity. Three parallel cultures of logarithmically growing HeLa cells were labeled with the same concentration of [^{3}H]methylmethionine, in media containing three different but known concentrations of cold methionine. At successive time intervals, samples containing cells at a known concentration were collected and the macromolecules precipitated at 0 °C by adding trichloroacetic acid to a final concentration of 10%. The samples were collected on glass fiber filters and counted in toluene scintillator. The endogenous methionine pool size per cell was calculated from the relative slopes of the three incorporation curves according to:

$$\frac{S_a}{S_b} = \frac{M_b + E}{M_a + E}$$

where S_i represents the slopes of the acid-precipitable methionine accumulation curve; M_i, the concentration of added methionine; and E, the effective concentration of endogenous methionine in the culture. (Thus E divided by the number of cells in the culture gives the effective endogenous methionine concentration per cell.)

Estimates of the effective [^{3}H]methylmethionine specific activity in subsequent experiments could thus be obtained. These calculations assume the rapid equilibration of the cellular methionine pool with exogenous methionine, an assumption born out by experimental results (see below).

Results

Experimental Design. The bulk of methylation has been reported to occur during or shortly after pre-rRNA transcription (Greenberg and Penman, 1966; Zimmerman and Holler, 1967) and all the methyl groups are conserved during processing (Maden and Salim, 1974). Thus methyl label is an excellent tracer for new rRNA, and any loss of methyl label that occurs between the 45S precursor, the known pre-rRNA intermediates, and the 28S and 18S products should be an accurate measure of any wastage that occurs.

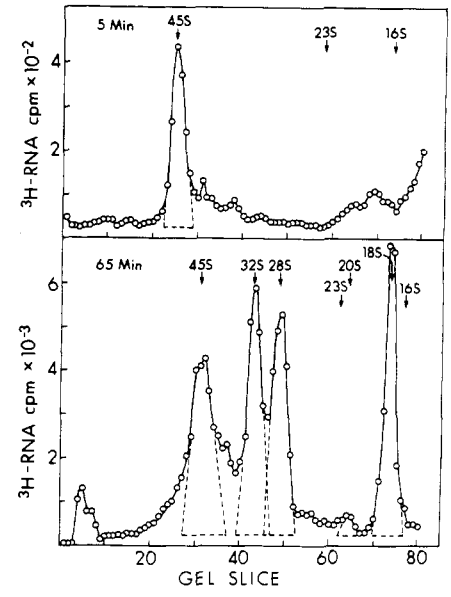

FIGURE 1: Polyacrylamide gel electrophoresis of [^{3}H]methyl labeled total cell RNA. Logarithmically growing culture of HeLa S3 cells was concentrated in methionine-free MEM Joklik supplemented with 5% dialyzed horse serum and incubated at 37 °C as described in Experimental Procedure. [^{3}H]Methylmethionine (3.7 Ci/mmol, 1 mCi/mL; Amersham/Searle) was added to 20 μCi/mL. Portions were withdrawn at the indicated times, the RNA was extracted, and specific activity was determined as described in Experimental Procedure. The patterns from a 5- and 65-min sample are shown. Arrows indicate the position of [^{14}C]uridine-labeled *E. coli* 23S and 16S rRNA coelectrophoresed with the HeLa cell RNA. A correction for the overlap of any ^{14}C counts into the ^{3}H channel has been made. The dotted lines indicate the extrapolated shape of the peaks and the background used in determining the counts in each species.

The accumulation of methyl label in each pre-rRNA and rRNA species was determined from polyacrylamide gel electrophoretic patterns of purified labeled total cellular RNA. The counts in each species of RNA at each time were estimated by summing the counts in the peaks of the corresponding gel and subtracting the background. Examples of the determinations are indicated in Figure 1. From the specific activity of the RNA (Experimental Procedure), the counts in each peak were then normalized to the amount of RNA added to the gel. Error estimates were obtained by calculating the counts in corresponding peaks from duplicate samples. The counts in each peak and for each time point were then divided by the known number of methyl groups in the appropriate species. A plot of the resulting values as a function of time for each species of RNA gives the relative moles of the species as a function of time (as in Figures 2 and 3).

The results, quantitated as described above, were analyzed using a simulation, analysis, and modeling program (SAAM 23; Berman, 1966), as follows. Analyzing the kinetics to determine the rates of formation, steady-state levels, and possible wastage would be impossible if the data for a single precursor were used as the only source of information for the accumulation curve of its product. This is because the experimental error and scatter of points is appreciable, and is especially marked for pools of small size, like 20S pre-rRNA. The SAAM 23 computer program, however, given the model, error esti-

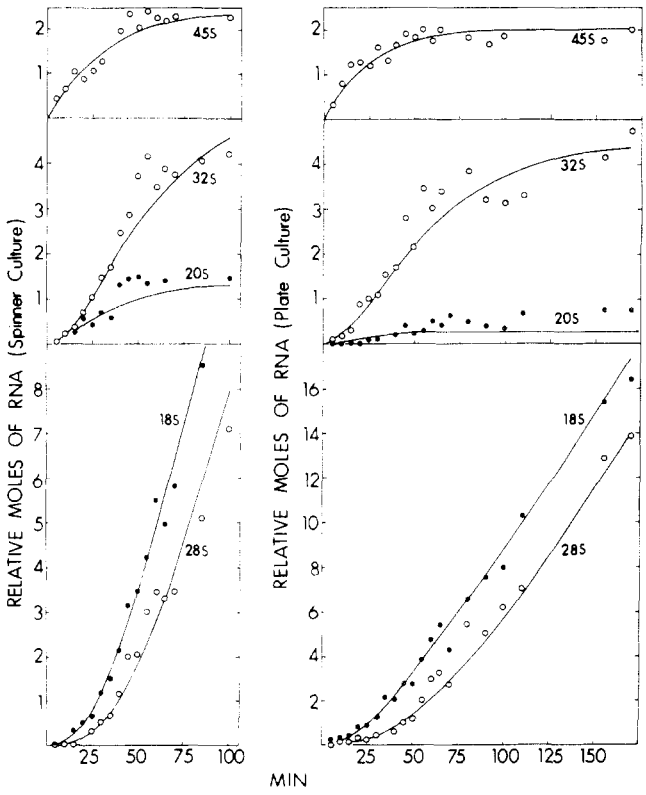

FIGURE 2: [^{3}H]Methyl-labeled pre-rRNA and rRNA accumulation curves in logarithmically growing HeLa S3 cells. (Left) A logarithmically growing spinner culture of HeLa S3 cells was treated as described in Figure 1. The accumulation curves were determined as described in the text and Experimental Procedure. Briefly, the total counts under peaks of each species of pre-rRNA and rRNA were determined for each gel (time point); gels were related to one another by normalizing to the μg of RNA applied to the gel; the total counts in each species were divided by the number of methyl groups in that species and the values plotted as shown. Thus the data represent the relative number of moles of each species of RNA as a function of time. Error estimates used in the analysis were 20% for the 45S, 32S, 28S, and 18S data points and 50% for the 20S data points. The drawn curves are the relative number of moles computed by the SAAM 23 program using model A (Table I). (Right) HeLa S3 cells, growing logarithmically on Petri dishes, were labeled as described in Experimental Procedure. The first six samples (set I) were labeled in medium containing 0.5 μg/mL cold methionine and 30 μCi/mL [^{3}H]methylmethionine (11 Ci/mmol, 1 mCi/mL); the next 11 samples (set II) were labeled in medium containing 2.0 μg/mL cold methionine and 30 μCi/mL [^{3}H]methylmethionine (11 Ci/mmol; 1 mCi/mL); and the last 7 samples (set III) were labeled in medium containing 5.0 μg/mL cold methionine and 40 μCi/mL [^{3}H]-methylmethionine (11 Ci/mmol, 1 mCi/mL). The accumulation curves were determined as described in Experimental Procedure. However, the relative specific activity curve used to normalize the counts in the pre-rRNA and rRNA species on the polyacrylamide gels was arrived at by adjusting the measured specific activities of the first set of plates and the third set of plates to the second set of plates, using the ratio of the slopes of the measured specific activity curves for each set of plates. The relative specific activity of a sample in set X = AB/C, where A is the measured slope of specific activity of set II; B is the measured specific activity of a sample in set X; and C is the measured slope of specific activity of set X. Error estimates used in the analysis were 30% for the 45S, 32S, 28S, and 18S data points and 50% for the 20S data points. The drawn curves are the relative number of moles computed by the SAAM 23 program using model A (Table I).

mates for each determination, and initial conditions, fits all of the accumulation curves simultaneously. Thus an analysis of the data is possible that yields much smaller estimates of probable error for most transitions despite the deviations in the individual precursor pools.

Based on the assumption of stochastic processing, the program obtains a least-squares fit to the data for each pathway

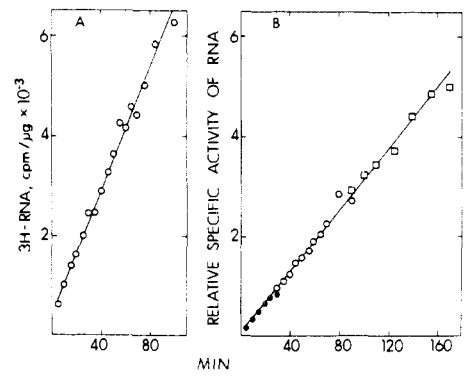

FIGURE 3: Incorporation of [^{3}H]methyl into RNA. (A) Cultures of HeLa S3 cells growing in spinner culture were labeled with [^{3}H]methylmethionine as described in Figure 1. Aliquots were withdrawn at the indicated times, the RNA was extracted, and specific activity was determined as described in Experimental Procedure. (B) HeLa S3 cells, growing logarithmically on Petri dishes, were labeled as described in Experimental Procedure and Figure 2 (right panel). The specific activity of the RNA from each set of plates was calculated as described in Experimental Procedure and Figure 2. (—●—) Set I; (—○—) set II; (—□—) set III.

in the model, rate constants for each transition, the standard deviation of each rate constant, and a table of the calculated values which correspond to the experimentally measured points. For our experiment, the program simultaneously solves a series of first-order linear differential equations of the form:

$$\frac{dq_a(t)}{dt} = \sum_b \lambda_{ab} q_b(t) - \sum_c \lambda_{ca} q_a(t)$$

In this relation, $q(t)$ for each species ($q_a(t)$, $q_b(t)$ . . .) represents that species content of radioactivity as a function of time, expressed in relative moles (cpm in the species at time t/number of methylated bases in the species). λ_{ab} represents the rate constant for processing of material from species "b" into species "a" (i.e., $\lambda_{ab}q_b(t)$ is the actual rate in relative moles per minute at which labeled molecules of RNA in species "b" are processed into labeled molecules in species "a" at time t). Thus the net rate at which label accumulates in any species (dq_a/dt) is given by the difference between the rates of formation of "a" from all pathways ($\Sigma_b \lambda_{ab} q_b(t)$) and rates of processing of "a" into all pathways ($\Sigma_c \lambda_{ca} q_a(t)$).

The experimental values for $q_a(t)$, $q_b(t)$, $q_c(t)$, etc. are determined from the acrylamide gel patterns as described above. λ's are initially estimated by the user and then adjusted by the program to obtain the best fit of the calculated q's to the experimentally determined values.

The approach to steady-state analysis, coupled with the use of [^{3}H]methylmethionine, circumvents several problems which complicate analysis using other precursors or a pulse-chase protocol. First, in contrast to pulse-chase experiments, the approach to steady-state labeling protocol allows one to determine the RNA half-lives, pool sizes, and RNA methyl contents under nearly normal physiological conditions. Second, [^{3}H]methylmethionine equilibrates with the cellular pool of methionine almost instantaneously. Figure 3 shows that the specific activity of extracted RNA from cells labeled either in spinner cultures or in Petri dishes began to increase linearly after no more than 5 min (the limit of resolution), and remained linear throughout the course of a typical experiment.

The resolution is further increased over trials with ^{3}H-labeled bases because the background of incorporation into HnRNA and mRNA is lower, since they are methylated to

TABLE I: Models for Processing of pre-rRNA and Formation of rRNA.

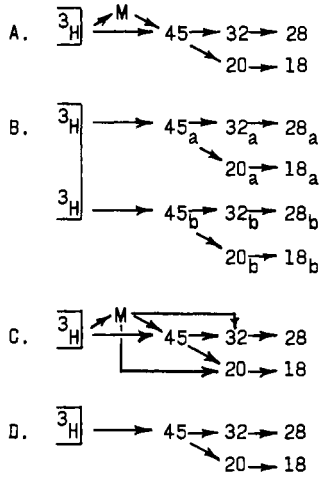

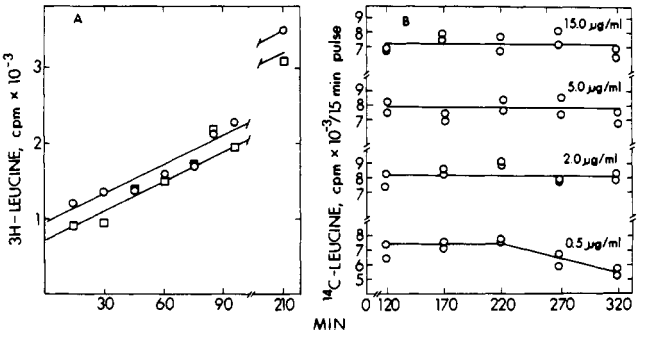

FIGURE 4: Incorporation of radioactive leucine into protein. (A) A logarithmically growing suspension culture of HeLa S3 cells was concentrated in methionine-free MEM Joklik supplemented with 5% dialyzed horse serum divided into two parallel cultures and incubated at 37 °C as described in Experimental Procedure. At time zero, cold L-methionine was added to the concentrations shown and [4,5-^{3}H]leucine (51 Ci/mmol, 0.5 mCi/mL; Schwarz/Mann) to 5.8 μCi/mL. Aliquots from each culture were withdrawn at the indicated times and labeled material was precipitated in ice-cold 10% trichloroacetic acid. The acid-insoluble material was collected on glass fiber filters and counted in a Packard TriCarb scintillation counter. Methionine concentration: (—○—) 15 μg/mL; (—□—) 1 μg/mL (15 μg/mL is the normal concentration of methionine in MEMα). (B) HeLa S3 cells, maintained in log phase growth in T flasks, were prepared as described in Experimental Procedure. The cells were pulse labeled for 15 min in the appropriate media containing [^{14}C]leucine (2.27 mCi/mg, 0.1 mCi/mL) at a concentration of 0.01 mCi/mL, at 120, 170, 220, and 320 min after the cells were shifted to medium containing the concentrations of cold methionine shown. Labeled cells were rinsed with ice-cold solution A, scraped off the plates with a rubber policeman, and resuspended in 2 mL of ice-cold solution A. Labeled material was precipitated in ice-cold 10% trichloroacetic acid, collected on glass fiber filters, and counted in a Packard TriCarb scintillation counter.

only about 1/6 the level of pre-RNA and rRNA (Brown and Attardi, 1965; Greenberg and Penman, 1966; Perry et al., 1970; Perry and Kelley, 1974).

Controls. The use of [^{3}H]methylmethionine required that cells be labeled in medium containing relatively low levels of methionine. In all experiments, the cells appeared to remain normal by several criteria: (1) the specific activity of extracted RNA (cpm/optical density unit) increased linearly from the first point measured (for example, Figure 3); (2) control experiments showed that cells growing in low methionine medium in spinner cultures accumulated [^{3}H]leucine into acid-insoluble protein at a normal rate for at least 210 min (Figure 4A); and similarly, cells grown in monolayers incorporated [^{14}C]leucine into acid-insoluble protein at a normal rate for at least 320 min in medium containing as little as 2.0 μg/mL cold methionine (Figure 4B); and (3) cells examined in a phase contrast microscope before and after the experiment showed normal cellular and nuclear morphology.

In experiments with cells growing in Petri dishes, all manipulations were done in a closed hood maintained at 37 °C, 5% CO_2, and 80% relative humidity. Small volumes of labeling medium could be used per Petri dish, with higher concentrations of labeled and unlabeled methionine than in spinner cultures. It therefore became unnecessary to concentrate the cells by centrifugation and resuspension in low methionine medium (see Experimental Procedure).

Under these conditions, no significant change in the incorporation of [^{3}H]methylmethionine into RNA was seen in 15-min pulses 2 or 5.5 h after shifting the cells to various low methionine media. For example, at 0.5, 5.0, and 15.0 μg/mL methionine, the specific activity of RNA from cells labeled for 15 min with [^{3}H]methylmethionine at a concentration of 60 μCi/mL (11 Ci/mmol) 2 h after shifting to the low methionine medium was 2050, 305, and 140 cpm/μg RNA, respectively. Five and one-half hours after the shift, a parallel set of cells labeled in the same way yielded RNA with specific activities of 2350, 360, and 140 cpm/μg RNA. As expected, no variation in the relative [^{3}H]methylmethionine labeling kinetics of the pre-rRNA and rRNA species was seen in monolayers labeled in media containing different concentrations of methionine (data not shown).

Several types of experiments indicated that little if any processing or aggregation of RNA took place during collection and extraction of cells. For example, when cells in spinner culture were labeled for a short period of time, only 45S pre-rRNA (and 18S rRNA, due to "late" methylations; Maden and Salim, 1975) was appreciably labeled (Figure 1). Also, in some trials, purified labeled 45S pre-rRNA was added to unlabeled cells and reextracted under various conditions; in the conditions used, the RNA showed the same profile before and after mixing with unlabeled cells and reextraction in phenol-detergent.

Models for Processing of Pre-rRNA. As mentioned above, the SAAM computer program obtains a least-squares fit to the data, given the error estimates and model for processing of the RNA. The major limitation is the selection of an appropriate model. Table I shows the four models which yielded a reasonable fit to the data.

Two criteria were used in determining the model which fit the data best: (1) models were sought which minimized the sum of squares of the deviations of the calculated values from the observed values. There is no statistical test to determine what the minimum sum of squares should be for a perfect fit to a given set of data. The minimum can only be arrived at through trial and error and comparisons of the observed "fit" for different models. (2) The fit was judged by the randomness of the scatter of the data points around the calculated curves. The "fitness" can be quantitated to some extent by summing the deviations of the observed from the calculated values. For points randomly scattered around the calculated curve, this sum should approach zero. However, in analyzing the data, the SAAM program fits four to five accumulation curves simultaneously. Therefore, in picking the model which gives the best fit, it becomes important to consider all the curves. Some models keep the total sum of squares low by improving the fit of one of the curves at the expense of the fit of one or several of the others.

TABLE II: Half-Lives of Processing Steps for Pre-rRNA.

Path	Experiment 1 $T_{1/2}$ (min)	2 $T_{1/2}$ (min)	3 $T_{1/2}$ (min)
M→45	17 ± 49%	8 ± 44%	24 ± 113%
45→32	10 ± 5%	11 ± 9%	11 ± 18%
32→28	21 ± 6%	30 ± 10%	25 ± 10%
20→18	5 ± 12%	2 ± 77%	2 ± 15%

TABLE III: Relative and Absolute Pool Sizes of Pre-rRNA and rRNA Species.

Experiment[a] / Model Pool	1 A	2 A	3 A
	Pool Size Relative to 32 S		
M	0.25 ± 15%	0.12 ± 13%	0.17 ± 85%
45	0.46 ± 15%	0.36 ± 13%	0.44 ± 18%
32	1.00 ± 15%	1.00 ± 13%	1.00 ± 18%
20	0.25 ± 15%	0.06 ± 13%	0.06 ± 18%
28	71 ± 15%	55 ± 13%	60 ± 18%
18	71 ± 15%	55 ± 13%	60 ± 18%
	Absolute Pool Size		
M	33 000 ± 40%	15 000 ± 40%	15 000 ± 20%
45	59 000 ± 40%	40 000 ± 40%	39 000 ± 20%
32	129 000 ± 40%	122 000 ± 40%	89 000 ± 20%
20	33 000 ± 40%	7 000 ± 40%	6 000 ± 20%
28	9×10^6 ± 40%	7×10^6 ± 40%	5×10^6 ± 20%
18	9×10^6 ± 40%	7×10^6 ± 40%	5×10^6 ± 20%

[a] Estimates are shown for two experiments with spinner cultures (1 and 2) and one with plate cultures (3)

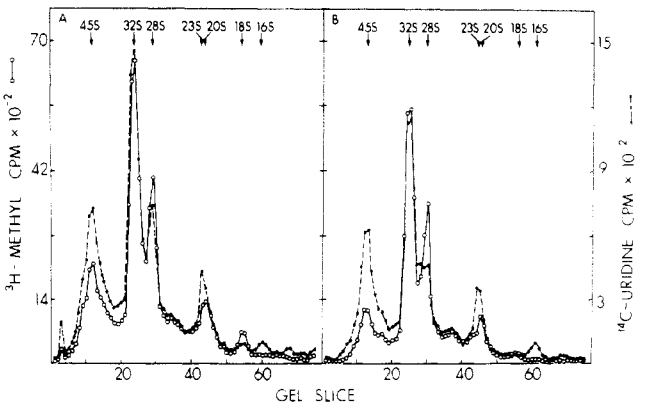

FIGURE 5: Polyacrylamide gel electrophoresis profiles of [^{3}H]methyl- and [^{14}C]uridine labeled nucleolar RNA. (A) HeLa S3 cells growing logarithmically in a pair of 250 cm^2 T flasks (approximately 5×10^7 cells per T flask) were washed, preincubated for 1 h, and labeled for 4 h as described in Experimental Procedure. In this case methionine was added to the medium to a final concentration of 15 μg/mL and cold uridine to 100 μg/mL (enough uridine to ensure linear incorporation of labeled uridine for 8 h). The volume of medium used to wash, preincubate, and label the cells was increased sixfold over experiments on Petri dishes to compensate for the larger number of cells. The labeling medium contained [^{3}H]-methylmethionine at 80 μCi/mL (10.5 Ci/mmol) and [2-^{14}C]uridine at 0.005 μCi/mL (55 Ci/mol; Amersham). Nucleoli were isolated essentially according to the method of Penman (1966) and the nucleolar RNA was purified and electrophoresed as described in Experimental Procedure. (B) HeLa S3 cells were grown and prepared in parallel to those described above except the preincubation and labeling medium contain cold methionine at a concentration of 5 μg/mL (enough to ensure linear incorporation of labeled methionine for 5 h). The nucleolar fractionation, RNA purification, and gel electrophoresis were done in parallel with the sample described in A.

Not surprisingly, for all three experiments, model A of Table I (or model A with a low level of wastage of 20S pre-rRNA) yielded the best fit to the data (see Discussion). As an example, the RNA accumulation data from experiments 1 and 3, along with accumulation curves representing the best computer fit to the data, are shown in Figure 2. Besides fitting the data well, model A is of course very close to the accepted sequence for rRNA maturation (Weinberg and Penman, 1970; Maden, 1971). It differs only in leaving out the small and difficult to measure pool of "41S pre-rRNA", and in the suggestion of a possible second precursor to complete 45S pre-rRNA (see below). All the data are consistent with stochastic rate-limiting steps, as assumed in the modeling, though very rapid ($\ll T_{1/2}$) ordered events might occur in any precursor pool. The analysis is thus effective in accurately determining and quantitating the nuclear and cytoplasmic events involved in rRNA synthesis.

Computed Half-Lives and Steady-State Pool Sizes of the Pre-rRNA Species. The results computed by the SAAM program, using the data from each of three experiments with model A (Table I), were used to calculate the half-lives for processing of each of the pre-rRNA species. These results are given in Table II. The absolute values for the time to make 28S rRNA or 18S rRNA (about 35 min and 12 min in experiment 1) are more precise, but similar to the qualitative estimates from earlier studies with uridine or methyl labeling (Penman et al., 1966; Greenberg and Penman, 1966).

Table III summarizes the calculated relative steady-state pool sizes for each of the major pre-rRNA species within a HeLa cell. It also lists the absolute steady-state pool sizes, calculated from the relative values and an estimate of the specific activity of the methionine during labeling.

To verify the relative pool sizes of 45S, 32S, and 20S inferred from the kinetic analysis, the relative amounts were assessed independently and directly by pulse labeling HeLa cell nucleolar RNA until all the pre-rRNA species were saturated. The gel electrophoretic profile of the nucleolar RNA shown in Figure 5 yields a pool size relative to 32S of 0.45 and 0.31 for 20S pre-rRNA. These results agree well with the relative pool sizes calculated using Model A (Table III). They are also within the range of literature values (cf. Weinberg et al., 1967, Figure 1; Weinberg and Penman, 1968, Table I).

In another test of the analysis, the inferred number of ribosomes per cell (Table III) was compared with a direct measurement. The number of ribosomes per HeLa cell was determined from the RNA content per cell, 80% of which was recovered as ribosomal RNA in gel analyses. A value of 9.5×10^6 ribosomes per HeLa cell in spinner culture was obtained, which agrees well with the estimated number of ribosomes per HeLa cell indicated in Table III.

The data of Table III also yield estimates that 1.4% of about 8×10^6 sequences of rRNA in actively growing HeLa cells is in the form of pre-rRNA species.

Wastage with Different Levels of Methylation. In all trials with actively growing cells, the rate constants for any wastage of pre-rRNA were set to zero or near zero by the computer analysis. In a few cases, a wastage term could have an appreciable value, but with a much higher sum of squares or a considerably worse fit to the data. Even when a small amount of wastage was consistent with the data, it would occur at the 20S

rRNA level, subsequent to initial processing. In other words, in logarithmically growing cells, every methyl group that enters 45S pre-rRNA arrives in 32S and 20S pre-rRNA species, and at least 90%—more likely 100%—arrives in completed 28S and 18S rRNA.

One unexpected "prediction" was made by the kinetic analysis. Consistently, a fraction of apparently slowly methylated 45S pre-rRNA was detected as an additional part of the precursor pool (see Discussion). Direct assay confirmed the existence of some undermethylated 45S pre-rRNA (Figure 5B). In cells labeled with [^{3}H]methylmethionine for 4 h in medium containing 5.0 μg/mL methionine, the methylation of 45S relative to 32S pre-rRNA decreased as compared with the control. The [^{14}C]uridine labeling pattern, however, showed no change. These trials indicate that, despite undermethylation of 45S pre-rRNA, proportionally normal levels of 32S and 20S pre-rRNA, as measured by uridine labeling, can be maintained in nucleoli.

Since slowly methylated pre-rRNA, as well as fully methylated pre-rRNA, is processed without detectable wastage in these cells, one could ask just how far methylation could be depressed without attendant wastage. As an extreme case, methionine was replaced with ethionine as completely as possible. Conditions were used in which protein synthesis and RNA synthesis, measured by radioactive leucine and uridine incorporation, nevertheless continued at normal rates for at least 2 h, and at least at 60% of normal rates for 3 more h. Figure 6 shows that under these conditions 45S pre-rRNA was formed at comparable rates in drug-treated and untreated cultures; but wastage in the ethionine-treated cultures was appreciable (about 85%).

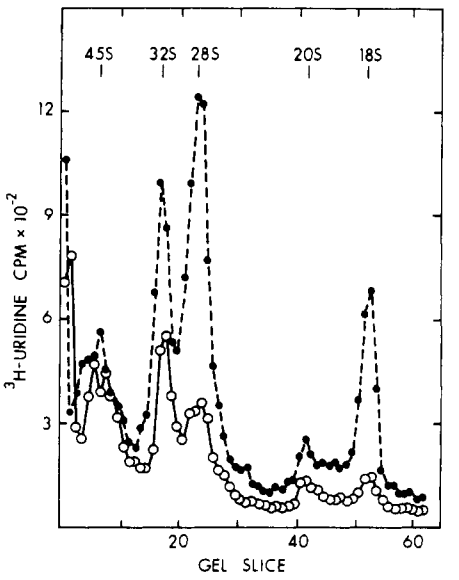

FIGURE 6: Accumulation of 45S and 32S pre-rRNA in the presence of ethionine. Parallel HeLa S3 cell cultures in log growth on 60-mm Petri dishes were prepared as described in Experimental Procedure. The cultures were preincubated for 1.5 h and then labeled for 2.5 h in medium containing [^{3}H]uridine (29 Ci/mmol) at a concentration of 20 μCi/mL and cold uridine at a concentration of 100 μg/mL. RNA purification and electrophoresis were as described in Experimental Procedure. For one culture (●--●), the preincubation and labeling medium contained methionine at a concentration of 15 μg/mL, while the preincubation and labeling medium of the second culture (○—○) contained no methionine but rather ethionine at a concentration of 163 μg/mL.

Discussion

Most of the results obtained in this study are confirmatory; they show that the modeling method works to require the pathway of RNA formation already well-accepted, and refines some previous qualitative estimates (particularly since analyses at many more times were done in kinetic trials compared with previous reports). The potential power of the method is, however, indicated by the way in which it sharpens estimates of nuclear wastage and kinetic constants; and by its detection of a slowly methylated, nonwasted fraction of precursor to 45S pre-rRNA even in exponentially growing cells. Some additional analysis of the connection between methylation, processing, and wastage has resulted. Here the present results are discussed further, and the flexibility that the approach may have to analyze rRNA metabolism in complex cases is briefly assessed.

Wastage of Nucleolar Pre-rRNA. Abelson et al. (1974) have shown that ribosomal RNA in the cytoplasm of growing cells turns over slowly or not at all, while Cooper (1973) has shown that, in nongrowing lymphocytes, "wastage" of 28S RNA occurs late in ribosomal maturation. Our results extend the observation of absence or near absence of rRNA turnover in growing cells to all the newly synthesized nuclear precursors. In HeLa cells growing logarithmically, either in spinner cultures or on plates, no degradation of 45S or 32S pre-rRNA was detected, and little or no wastage of 20S pre-rRNA was observed. The significance of the computer analysis in reaching these conclusions is important to note. The interdependent fitting of the accumulation curves of each of the pre-rRNA and rRNA species yields much smaller error estimates for the computed fraction of RNA wasted at each processing step. This would be impossible if data for individual RNA species, with larger probable errors, could only be analyzed independent of data for the other species.

A very rapid turnover of some rRNA transcripts following on the heels of their synthesis is impossible to exclude with the kinetic analysis, because these chains would never be seen. However, in conditions where methionine was limiting, unmethylated pre-rRNA could accumulate for some time without being degraded (see below). It thus seems less likely that any fully methylated normal transcripts would be degraded.

Undermethylation and the Relation of Pre-rRNA Methyl Content to Processing. The possible significance of methylation in relation to RNA processing has often been considered. Earlier reports (Zimmerman and Holler, 1967; Vaughan et al., 1967) have shown that the appearance in the cytoplasm of newly synthesized rRNA is dependent on methylation (although under stringent conditions of methionine starvation, 45S pre-rRNA can still be processed, at least in part, to 32S pre-rRNA (Vaughan et al. 1967)). Our results suggest that the required methylations need not occur concomitantly with transcription and, in fact, that, in cells maintained in medium containing nearly normal concentrations of methionine, a significant fraction of the 45S pre-rRNA pool is undermethylated.

Our first suggestion of some unmethylated 45S pre-rRNA came from the kinetic analyses. The "fit" of the computed accumulation curves in all experiments was aided by the introduction of a precursor pool of unmethylated RNA (pool M) to adjust for a relatively slow appearance of some methyl label in 45 S. For example, using model D of Table I (which excludes pool M) led to a twofold higher sum of squares for the data of experiments 1 and 2. When used in analyzing the data of experiment 3, the same model led to a sum of squares only 6% higher, but to a worse fit of the data to the calculated curves.

A straightforward interpretation suggests that a small but

variable sized pool of transiently unmethylated 45S pre-rRNA may exist in logarithmically growing HeLa cells (Table III). (As an alternative, pool M may represent a difference in methylation and processing rates in a subfraction of the cellular or nucleolar populations. However, for two parallel pathways with different rate constants (Model B, Table I), the fit to the data was not as good as that for one pathway which included pool M.)

Direct assay confirmed the existence of an undermethylated 45S pre-rRNA pool (Figure 5B). Cells grown in higher concentrations of methionine may not exhibit undermethylated 45S pre-rRNA. However, this is the first case, to our knowledge, in which any undermethylated rRNA has been detected in rapidly growing cells.

Nevertheless, RNA tends to be methylated before it is processed. This was suggested by tests of model C (Table I), which allows processing of pool M RNA to the 32S and 20S level without its prior appearance as methylated 45S pre-rRNA. Model C was not consistent with the data. In experiment 2 the rate constant for processing pool M RNA to 32S and 20S RNA was set equal to zero by the SAAM program. Similarly, in experiment 1, when model C was used, the rate constant was set to a very small value (more than tenfold lower than the 45S to 32S or 45S to 20S rate constants), essentially converging to model A. In experiment 3, model C led to a similar "sum of squares" relative to model A but to a worse fit as indicated by the "fitness" of the 45S, 32S, and 28S pools. In addition, the calculated relative pool sizes of 32S and 45S pre-rRNA did not agree well with independent determinations.

The notion has been widely accepted that methyl groups are critical for complete maturation of rRNA. However, as Warner (1974) has summarized, the inference has come primarily from experiments with cells starved from amino acids (e.g., Vaughan et al., 1967). In such cases, protein synthesis is of course sharply curtailed; and since agents which block protein synthesis also force wastage (like puromycin; Latham and Darnell, 1965; Soeiro et al., 1968) without affecting methylation, it has been unclear whether methionine deprivation leads to wastage because of a failure of protein synthesis or because of a failure of methylation.

To extend the analysis somewhat further, the analog ethionine was used here. In early studies, ethionine was found to cause a sharp depletion of the cellular ATP pool; but under appropriate conditions (Winston, 1973) cellular ATP levels remain normal. In *E. coli* so treated with ethionine, protein synthesis and ribosome formation proceed at near-normal rates, with the formation of inactive ribosomal particles that become methylated and active when methionine is restored to the medium (or to extracts; Alix and Hayes, 1974).

In HeLa cells, protein synthesis continues at a rate comparable to controls, and the 45S pre-rRNA is formed at a near normal rate for hours (Figure 6 and unpublished data; quantitative studies have shown a similar result with puromycin). However, in contrast to the results with bacteria, processing is arrested after initial cleavage of the 45S pre-rRNA, and it is then largely wasted (Figure 6). These results support the importance of methylation for rRNA maturation; though as an alternative, it has still not been excluded that certain ethionine-substituted proteins in HeLa cells may not be as functional as comparable proteins in *E. coli*.

From the kinetic analysis and independent experiments it thus appears that methylation is not absolutely necessary for initial processing, although the probability of initial processing is enhanced for RNA which has been methylated.

One possibility is that a particular conformational change is required to expose sites both for cleavage and for methylation of nucleolar pre-rRNA. Methylation thereafter does become critical, and any RNA that is further processed without methylation is increasingly subject to wastage.

Extensions of the Analysis. The refinement of kinetic constants (Tables II and III) and pre-rRNA processing models, which led to the detection of slowly methylated pre-rRNA in growing cells, provides some indication of uses of the modeling analysis. It motivated the study of ethionine-treated cells, though the results in that case are so extreme that the result is clear without computer analysis (Figure 6)!

Comparable analyses of precursor relationships should be possible for RNA in cells in a number of physiological states: for example, in some cases, an unambiguous pathway for rRNA maturation has not been found by simple labeling analysis; in others, a larger precursor than the "initial" one seen has been suggested; and in lymphocytes, wastage has been suggested by some but not other authors. We will report elsewhere on the use of the analysis to study rRNA metabolism in nongrowing and "crisis"-phase human diploid fibroblasts.

Acknowledgments

We thank Dr. Sadao Gotoh and Dr. Bratin Saha for helpful discussions during the course of this work. We also thank the Anatomy Department of Washington University Medical School for the use of their computer in processing the data and Rich Wren for aid in writing the processing program.

References

Abelson, H. T., Johnson, L. F., Penman, S., and Green, H. (1974), *Cell 1,* 162–165.

Alix, J. H., and Hayes, D. (1974), *J. Mol. Biol. 86,* 139–159.

Berman, M. (1966), Users Manual For SAAM (simulation, analysis, and modeling), Washington, D.C., Government Printing Office, catalogue number 5562.

Berman, M., Shahn, E., and Weiss, N. F. (1962), *Biophys. J. 2,* 275–287.

Brown, G. M., and Attardi, G. (1965), *Biochem. Biophys. Res. Commun. 20,* 298–302.

Cooper, H. L. (1973), *J. Cell Biol. 59,* 250–254.

Cooper, H. L., and Gibson, E. N. (1971), *J. Biol. Chem. 246,* 5059–5066.

Dische, Z. (1953), *J. Biol. Chem. 204,* 983.

Greenberg, M., and Penman, S. (1966), *J. Mol. Biol. 21,* 527–535.

Latham, M., and Darnell, J. E. (1965), *J. Mol. Biol. 14,* 13–22.

Maden, B. E. H. (1971), *Prog. Biophys. Mol. Biol. 22,* 127–177.

Maden, B. E. H., and Salim, M. (1974), *J. Mol. Biol. 88,* 133–164.

Maden, B. E. H., Salim, M., and Summers, D. F. (1972), *Nature (London), New Biol. 237,* 5–9.

Penman, S. (1966), *J. Mol. Biol. 17,* 117–130.

Penman, S., Smith, I., and Holtzman, E. (1966), *Science 154,* 796–799.

Perry, R. P., Cheng, T.-Y., Freed, J. J., Greenberg, J. R., Kelley, D. E., and Tartof, K. D. (1970), *Proc. Natl. Acad. Sci. U.S.A. 65,* 609–616.

Perry, R. P., and Kelley, D. F. (1974), *Cell 1,* 37–42.

Soeiro, R., Vaughan, M. H., and Darnell, J. E. (1968), *J. Cell*

Biol. 36, 91-101.
Toniolo, D., Meiss, H. K., and Basilico, C. (1973), *Proc. Natl. Acad. Sci. U.S.A. 70,* 1273-1277.
Vaughan, M. H., Jr., Soeiro, R., Warner, J. R., and Darnell, J. E., Jr. (1967), *Proc. Natl. Acad. Sci. U.S.A. 58,* 1527-1534.
Warner J. R. (1974), in Ribosomes, Nomura, M., Tissières, A., and Lengyel, P., Ed., Cold Spring Harbor, N.Y., Cold Spring Harbor Laboratory, pp 461-488.
Weinberg, R. A., Leoning, U., Willems, M., and Penman, S. (1967), *Proc. Natl. Acad. Sci. U.S.A. 58,* 1088-1095.
Weinberg, R. A., and Penman, S. (1968), *J. Mol. Biol. 38,* 289-304.
Weinberg, R. A., and Penman, S. (1970), *J. Mol. Biol. 47,* 169-178.
Winston, A. J. (1973), *Chem.-Biol. Interact. 7,* 272-282.
Zimmerman, F. F., and Holler, B. W. (1967), *J. Mol. Biol. 23,* 149-161.

Formation of Products of the 5,6-Dihydroxydihydrothymine Type by Ultraviolet Light in HeLa Cells†

P. V. Hariharan‡ and P. A. Cerutti*

ABSTRACT: The formation of products of the 5,6-dihydroxydihydrothymine-type (t^{UV}) and cyclobutane-type pyrimidine photodimers (TT) and tritiated water (^3H_2O) by monochromatic light at 240, 265, 280, and 313 nm (6-nm half-bandwidth) was investigated in HeLa S-3 cells which were labeled in their DNA with [*methyl*-^{3}H]thymine. The efficiency of the formation of all three products was maximal at 280 nm and dropped towards longer and shorter wavelengths. The efficiency of TT formation dropped more strongly towards longer and shorter wavelengths than the efficiency of t^{UV} formation (comparison at a dose of 5×10^3 J m^{-2}). Total monomeric thymine ring saturation (t_{sat}) was estimated from the t^{UV} data. It was calculated that 0.06 t_{sat} was formed for each TT at 280 nm, but 0.73 t_{sat} per TT at 313 nm. It follows that monomeric thymine ring saturation represents a minor photochemical reaction relative to pyrimidine dimerization in the far-ultraviolet but a major reaction in the near-ultraviolet. The formation of ^3H_2O by ultraviolet light from [*methyl*-^{3}H]thymidine-labeled HeLa cells most likely indicates the attack of hydroxyl radicals on the cellular DNA; 5-methyleneuracil radicals formed as a consequence of the reaction may be important intermediates in ultraviolet-induced DNA-DNA and DNA-protein cross-linking.

Cyclobutane-type pyrimidine dimers are the major lesions produced in the DNA of bacteria and mammalian cells by far-ultraviolet light (far-UV,[1] <300 nm). They are responsible for most of the killing and mutagenic action of far-UV. The formation of other lesions, in particular, of nondimeric ring-saturation products of thymine and cytosine, has been observed. Wacker (1963) described the formation of products other than photodimers in DNA irradiated at 254 nm and one of these products was later identified as 5,6-dihydrothymine (Yamane et al., 1967). The formation of small amounts of thymine photohydrate, 6-hydroxy-5,6-dihydrothymine, by 265-nm irradiation (Fisher and Johns, 1973) and of deoxycytidine photohydrate, 6-hydroxy-5,6-dihydrodeoxycytidine, in oligonucleotides and DNA at 254 nm (Vanderhoek and Cerutti, 1973) has been documented. Photooxidation of thymine to 5,6-dihydroxydihydrothymine by light of 184.9 and 254 nm to 5-hydroxymethyluracil, 5-formyluracil, and uracil has been investigated by Daniels and Grimison (1967) and by Alcantara and Wang (1965), respectively.

The photochemistry of DNA and its building blocks in the near-ultraviolet region (near-UV, 300-380 nm) is less well understood. Near-UV light is of particular interest to the environmental and medical sciences, since it is contained in the sun spectrum reaching the surface of the earth in contrast to far-UV which is mostly absorbed by the terrestrial ozone shield. Cyclobutane-type pyrimidine dimers are formed by near-UV but with much lower efficiency than by far-UV light (Tyrrell, 1973). Near-UV has been shown to produce alkali-labile bonds in DNA in situ in the cell but these lesions have not yet been chemically characterized (Tyrrell et al., 1974). Irradiation of thymine in solution in the presence of H_2O_2 with near-UV light leads to the formation of hydroperoxy derivatives of 5,6-dihydrothymine (Hahn and Wang, 1974).

We have undertaken a study of the formation of thymine photodimers and monomeric, ring-saturated thymine lesions of the 5,6-dihydroxydihydrothymine type (t^{UV}) in human carcinoma HeLa S3 cells upon irradiation with monochromatic light at 240, 265, 280, and 313 nm under aerobic conditions. We have also measured the formation of tritiated water from [*methyl*-^{3}H]thymidine-labeled cells which gives a measure of the photochemical reactivity of the methyl group of thymine. It was found that products of the 5,6-dihydroxydihydrothymine type represent minor lesions relative to pyrimidine photodimers in the far-UV but major lesions in the near-UV.

Materials and Methods

Growth of Cells and Radioactive Labeling. HeLa S-3 cells were grown at 37 °C, in spinner cultures and in Joklik's modified minimal essential medium, supplemented with cold thy-

† From the Department of Biochemistry and Molecular Biology, J. H. Miller Health Center, University of Florida, Gainesville, Florida 32610. *Received December 20, 1976.* This work was supported by USERDA Contract AT-(40-1)-4155.

‡ Present address: Department of Biophysics, Roswell Park Memorial Institute, Buffalo, N.Y. 14263.

[1] Abbreviations used are: UV, ultraviolet light; t^{UV}, products of the 5,6-dihydroxydihydrothymine type; t_{sat}, total monomeric, ring-saturation and ring-destruction products of thymine; TT, cyclobutane type pyrimidine photodimers containing one or two thymine moieties; 5′-TMP, thymidine 5′-monophosphate.